

## DYNAMICAL STUDY OF THE FLOW ALONG A TWO-DIMENSIONAL CHANNEL WITH A RIGHT ANGLED BEND

A. BRIMA<sup>1</sup>, R. ATMANI<sup>1</sup>, M. BENTERCIA<sup>2</sup> & B. ACHOUR<sup>3</sup>

<sup>1</sup>Department of Mechanics, University of Biskra, Algeria  
Research laboratory in Mechanical Engineering (LGM)

<sup>2</sup>Elkassim University, Arabian Saudi King Dom

<sup>3</sup>Department of Hydraulics, University of Biskra, Algeria  
Research laboratory in subterranean and surface Hydraulics (LARHYSS)  
E-mail: hafidd@hotmai.com

### ABSTRACT

A two-dimensional incompressible laminar flow passing through a constant width channel with a ninety-degree turn is investigated. Based on the flow separation and recirculation phenomena downstream of the inner corner, a model profile for the axial velocity component is chosen.

Concerning the channel segments upstream and downstream of the previous corner, the insertion of the velocity profiles (incorporating a distortion profile function) in the Navier-Stokes equations and the use of the integral method lead to a linear differential equation for the previous function. Whereas, the corresponding previous differential equation is not linear in the corner region. The analytical and numerical solutions for the first and last equations respectively are obtained and the Reynolds number  $Re$  as well as recirculation bubble effects on the flow variables are presented for  $(100 \leq Re \leq 540)$ ; the experimental range of flow visualisation and measurement).

**Keywords:** laminar flow, distortion function, velocity profile, flow separation, recirculation bubble.

### RESUME

L'écoulement incompressible, laminaire et bidimensionnel le long d'une conduite coudée à 90° a été étudié. En se basant sur le phénomène de séparation et de recirculation just après le coude, un modèle de profil de la composante de vitesse axiale est choisie. Concernant les deux parties en amont et en aval du coude, l'introduction du profil de vitesse (introduction du profil de la fonction de déformation) à l'intérieur des équations de "Navier Stocks" et l'utilisation de la méthode intégrale mènent à une équation différentielle linéaire dont l'inconnue est bien la fonction de déformation. Alors que, l'équation différentielle précédente est non linéaire au niveau du coude. Les solutions analytique et numérique respectivement pour la première et la dernière équation différentielle sont obtenues. L'effet du nombre de Reynolds aussi bien de la bulle de recirculation sur les variables de l'écoulement est présenté pour  $100 \leq Re < 540$  (plage expérimentale de mesure et visualisation).

**Mots clés:** écoulement laminaire, fonction de déformation, profil de vitesse, séparation de l'écoulement, bulle de recirculation.

### 1 INTRODUCTION

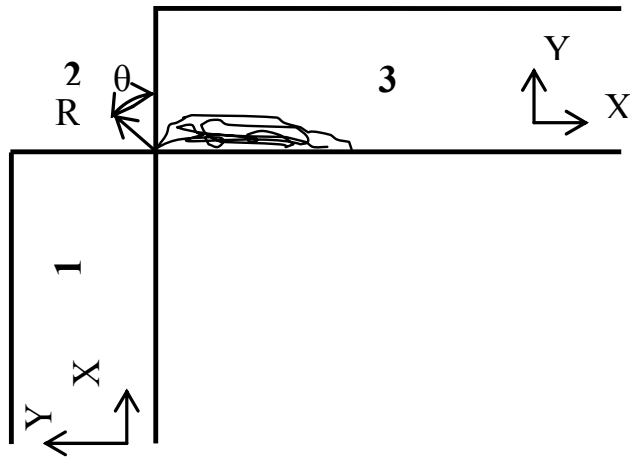
It is scarce to establish a fluid flow in any engineering equipment without bends, valves and bifurcations. Even the blood circulatory system includes such regions and devices. These geometries are behind many complicated flow phenomena such as: flow separation, recirculation and reattachment. The previous flow complications introduce many losses and lead to the performance drop for piping systems. For these reasons, it is important to analyse the flow behavior and determine the velocity as well as the

pressure distributions through these regions. Although the limiting case of a channel bending (a sharp 90 degree turn for the inner wall) is not very common in engineering flow systems, its consideration in this study illustrates much better the recirculating flow just downstream of the inner corner and its effects on the flow variables. However the same analysis is applicable to the ordinary bending provided that suitable boundary conditions at the bend entrance and exit have to be chosen.

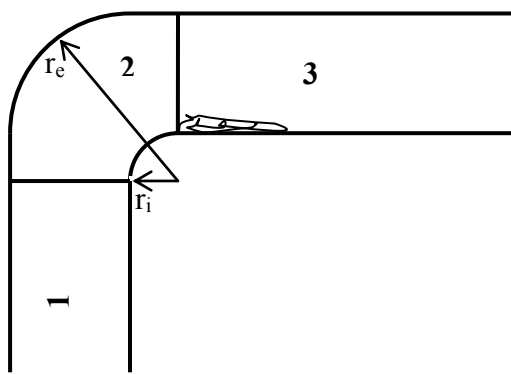
## 2 FORMULATION

In many engineering applications, the flow systems can be approximated by two-dimensional channels in which incompressible fluids circulate steadily and laminarily. This study is limited to a such type of the previous fluid flows and the two-dimensional channel presents two sorts of bending (a gradual turn and a sharp 90-degree turn), see fig.1.

Referring to the previous figure, the flow can be described by the following basic equations.



(a) miter-bend



(b) elbow

Figure 1 : Schematic mean flow through a bending channel:

(a) miter-bend, (b) elbow

### 2.1 Regions 1&3

The non-dimensional governing equations, given in Cartesian co-ordinates, are:

$$\frac{\partial U}{\partial X} + \frac{\partial V}{\partial Y} = 0 \quad (1)$$

$$U \frac{\partial U}{\partial X} + V \frac{\partial U}{\partial Y} = -\frac{1}{\rho} \frac{\partial P}{\partial X} + \frac{1}{\text{Re}} \left( \frac{\partial^2 U}{\partial X^2} + \frac{\partial^2 U}{\partial Y^2} \right) \quad (2)$$

$$U \frac{\partial V}{\partial X} + V \frac{\partial V}{\partial Y} = -\frac{1}{\rho} \frac{\partial P}{\partial Y} \quad (3)$$

Where  $\nabla^2 V$  is neglected in this last equation

### 2.2 Region 2

The non-dimensional forms of the previous equations, written in polar co-ordinates, are:

$$\frac{\partial}{\partial R} (RV) + \frac{\partial U}{\partial \theta} = 0 \quad (4)$$

$$V \frac{\partial V}{\partial R} + \frac{U}{R} \frac{\partial V}{\partial \theta} - \frac{U^2}{R} = -\frac{1}{\rho} \frac{\partial P}{\partial R} + \frac{1}{\text{Re}} \left[ \frac{\partial}{\partial R} \left( \frac{1}{R} \frac{\partial}{\partial R} (RV) \right) + \frac{1}{R^2} \frac{\partial^2 V}{\partial \theta^2} - \frac{2}{R^2} \frac{\partial U}{\partial \theta} \right] \quad (5)$$

$$V \frac{\partial U}{\partial R} + \frac{U}{R} \frac{\partial U}{\partial \theta} + \frac{VU}{R} = -\frac{1}{\rho} \frac{\partial P}{\partial \theta} + \frac{1}{\text{Re}} \left[ \frac{\partial}{\partial R} \left( \frac{1}{R} \frac{\partial}{\partial R} (RU) \right) + \frac{1}{R^2} \frac{\partial^2 U}{\partial \theta^2} + \frac{2}{R^2} \frac{\partial V}{\partial \theta} \right] \quad (6)$$

Concerning the specification of the boundary conditions, the division of the channel in the three regions introduces some difficulties about specifying the boundary conditions at the ends of each region. However, this complication can be burdened compared to the resulting simplification of the problem solution (obtaining of analytical solutions in regions 1&3).

The choice of the boundary conditions will be specified in details after the presentation of the solution method.

## 3 METHOD OF SOLUTION

The integral method which consists of integrating the basic equations across the channel is used. However, this step should be associated with a good assumption for the profiles of velocity components. In this analysis, the assumption of U-profile is inspired from the flow configuration just downstream of the miter-bend. In fact, the flow in this region experiences the biggest distortion (recirculation near the inner wall, acceleration outside the recirculation bubble and deceleration close to the outer wall in order to satisfy the non-slip conditions). This flow examination on one hand and the use of the continuity equation on the other hand lead to the following assumed profiles:

### 3.1 Region 1&3

$$U(X, Y) = F(Y) + Z(X)G(Y) = (Y - Y^2) + Z(X)(2Y^3 - 3Y^2 + Y) \quad (7)$$

and

$$V(X, Y) = -\left(\frac{dZ}{dX}\right)\left(\frac{Y^4}{2} - Y^3 + \frac{Y^2}{2}\right) \quad (8)$$

Where:

$Z(X)$  is a distortion function

The differentiation of eq.(2) with respect to  $Y$  and equation (3) with respect to  $X$  and the subtraction of the last resulting equation from the one before it gives:

$$\begin{aligned} & \frac{\partial U \partial U}{\partial X \partial Y} + \frac{U \partial^2 U}{\partial X \partial Y} + \frac{\partial V \partial U}{\partial Y \partial Y} + \frac{V \partial^2 U}{\partial Y^2} \\ & - \frac{\partial V \partial U}{\partial X \partial X} - \frac{U \partial^2 V}{\partial X^2} - \frac{\partial V \partial V}{\partial X \partial Y} - \frac{V \partial^2 V}{\partial X \partial Y} \\ & = \frac{1}{\text{Re}} \frac{\partial}{\partial Y} \left[ \frac{\partial^2 U}{\partial X^2} + \frac{\partial^2 U}{\partial Y^2} \right] \end{aligned} \quad (9)$$

Expressing each term in equation(9) in terms of the assumed profiles given in equation(7) & equation(8) and integrating the resulting equation across the channel (between  $Y=0$  and  $Y=1$ ), we get the following ordinary differential equation:

$$\frac{d^3 Z}{dX^3} - \frac{3360}{\text{Re}} Z = 0 \quad (10)$$

### 3.2 Region 2

Similarly, the following profiles for  $U$ & $V$  components are assumed:

$$U(R, \theta) = F(R) + Z(\theta)G(R) = (R - R^2) + Z(\theta)(2R^3 - 3R^2 + R) \quad (11)$$

$$V(R, \theta) = -\left(\frac{dZ}{d\theta}\right)\left(\frac{R^3}{2} - R^2 + \frac{R}{2}\right) \quad (12)$$

Following the above steps, used to obtain the equations (9) & (10) except that for a gradual bending we make a clever variable transformation [ $R=(r-r_1)/h$ ] instead of ( $R=r/h$ ) in order to keep the same integration limits ( $R=0$  &  $R=1$ ), we get the same following equation for both flow systems:

$$\begin{aligned} & \frac{1}{280} \frac{d^3 Z}{d\theta^3} - \frac{1}{12 \text{Re}} \frac{d^2 Z}{d\theta^2} + \frac{1}{210} \frac{dZ}{d\theta} - \frac{1}{210} Z \frac{dZ}{d\theta} \\ & - \frac{1}{560} \frac{dZ}{d\theta} \frac{d^2 Z}{d\theta^2} - \frac{3}{\text{Re}} Z + \frac{1}{\text{Re}} = 0 \end{aligned} \quad (13)$$

It is clear that the first gain from dividing the channel in three regions is the obtention of the linear differential equation(10) which can be solved analytically. Whereas, equation(13) is not linear and it can not be solved analytically unless a suitable drop of some non-linear terms is made. In order to solve the equations(10), (13) & (14) a set of boundary conditions has to be supplied.

Since the equations (10) & (13) are similar from the mathematical point of view ( they differ only in terms of the constant coefficients ), the solution will be presented only for the sharp 90 degree turn (limiting case for flow separation and recirculation).

Since the miter bend illustrates better the flow separation and recirculation phenomena, only the solution for this channel configuration is presented.

## 4 BOUNDARY CONDITIONS SPECIFICATION

The specification of the boundary conditions, in term of the distortion function  $Z$  and its derivatives, is deduced from the corresponding ones vis a vis the velocity components  $U$ & $V$ .

### 4.1 Region 1

The consideration of a fully developed flow for upstream of the bend signifies that:

$U$  profile is parabolic

- $Z(-\infty) = 0$

Also:

$V$ -component equal to zero

- $\frac{dZ}{dX}(-\infty) = 0$

At the bend entrance, we assume that the flow starts to deviate with a small angle towards the right.

$$\frac{V}{U} = \tan \beta (\text{with } \tan \beta \approx \beta)$$

$$\frac{dZ}{dX}(0) \approx 10 \tan \beta$$

#### 4.2 Region 2

The continuity of the velocity components at the entrance section gives:

- $Z(X = 0) = Z(\theta = 0)$
- $\frac{dZ}{dX}(X = 0) = \frac{Z(\theta = 0) - Z(\Delta\theta)}{\Delta\theta}$

At the bend exit, we use the flow separation condition at the inner corner

Shear stress at  $(Y = 0) = 0$  which corresponding to:

$$Z(\pi / 2) = -1$$

#### 4.3 Region 3

At the entrance of this region, we use again the continuity of the V-component and flow separation, there fore:

$$Z'(X=0)=0$$

- $Z(X = 0) = Z(\theta = \pi / 2) = -1$

Finally, the reestablishment of the fully developed flow for downstream of the bend is characterised by:

- U-profile is parabolic  $Z(\infty) = 0$

The application of the previous sets of the boundary conditions of the corresponding equations leads to the following solution for Z:

$$Z(\text{Re} = 148) = \begin{cases} 0.327 \exp(2.831X) & -\infty < X < 0 \\ 0.327 + 1.107\theta - 2.098\theta^2 + 0.553\theta^3 & 0 < \theta < \pi/2 \\ -\exp(-1.415X) [\cos(0.049X) + 69.62 \sin(0.049X)] & 0 < X < +\infty \end{cases}$$

$$Z(\text{Re} = 297) = \begin{cases} 0.412 \exp(2.244X) & -\infty < X < 0 \\ 0.412 + 1.121\theta - 2.257\theta^2 + 0.626\theta^3 & 0 < \theta < \pi/2 \\ -\exp(-1.122X) [\cos(0.038X) + 78.754 \sin(0.038X)] & 0 < X < +\infty \end{cases}$$

$$Z(\text{Re} = 539) = \begin{cases} 0.503 \exp(1.840X) & -\infty < X < 0 \\ 0.503 + 1.135\theta - 2.392\theta^2 + 0.683\theta^3 & 0 < \theta < \pi/2 \\ -\exp(-0.920X) [\cos(0.031X) + 89.143 \sin(0.031X)] & 0 < X < +\infty \end{cases}$$

In each bracket, the first and the last expressions correspond to the analytical solutions. Once the expressions of Z are obtained, their insertion in the U- & V-profiles allows to find their distribution across and along the channel. The variation of the pressure gradient along the inner and outer walls can be obtained through the momentum equations. The results are plotted in fig. 2, ..., fig. 8.

## 5 RESULTS AND CONCLUSION

Fig. 2 depicts the variation of the key function Z along the channel length. The profile pattern shows that this distortion function passes by a maximum negative value in the bubble region. This agrees with the fact that the biggest distortion in U-profile occurs in the previous region.

Concerning the departure of the U-profile along the channel length, Fig. 3 displays that the maximum values of the velocity is shifted slightly towards the inner wall at the entrance of the corner region. However the previous maximum point moves towards the outer wall as the fluid flows downstream and the negative values of this components appear once the flow enters in the bubble region as it is shown in Fig. 4. For the V-component, the results denote that it is almost negligible in region 1. However it reaches its highest value just after the flow separation  $(X = 0.1 \text{ \& } Y = 0.5)$  where the local flow deviation with respect to the channel centreline is maximum. The V-profile in the previous location is shown in Fig. 5. The previous distributions of the velocity components are also found in [2] & [3].

Now it remains to see how the U- component varies along the channel length, especially for the transversal distance which does not exceed the bubble height. Fig. 6 shows the distribution of the U- component along the channel length and for  $Y = 0.25$ , the bubble effect which manifests in the reversed flow is clear in this profile. The variations of the pressure gradient along the outer and inner walls of the channel are shown in Fig. 7 and Fig. 8 respectively. Comparing the profiles of Z and the pressure gradient along the outer wall we see that they are similar and this might be due to reduction of  $(dP/dX)_{\text{outer}}$  expression to  $(AZ+B)$  with  $A > 0$ , whereas the  $(dP/dX)_{\text{inner}}$  varies in inverse manner with respect to Z. This behavior is also reported in [4]. The last interesting variable is the bubble length. Table 1 shows both the computed (by the present solution) and measured [1] lengths. The agreement between both results is good. Concerning the secondary flow establishment, the consideration of two dimensional channel on one hand and the limitation of steady to a range of relatively low Reynolds number on the other hand make the occurrence of such flow unlikely [5].

Finally, we can conclude that the present model as reflected many flow features and provided an analytical solution at least in regions 1&3. Also the model can be extended to many other flow geometries with previous boundaries conditions, cavities, bifurcations.

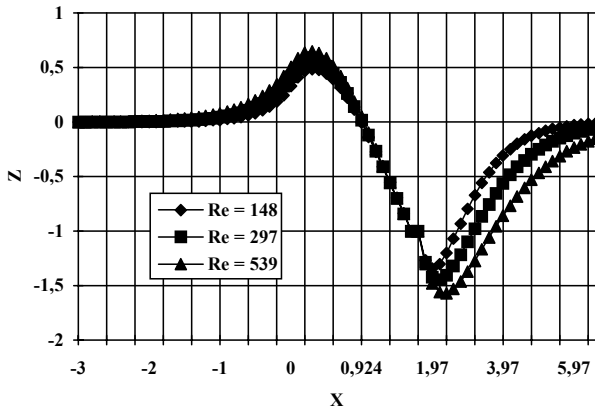


Figure 2 : Distribution of distortion function

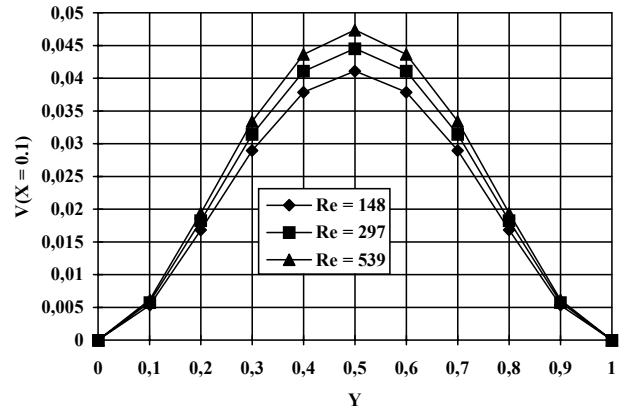


Figure 5 : Profile of V-component just after the inner corner

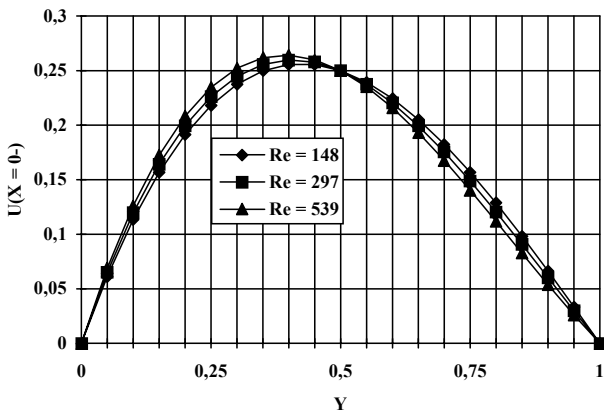


Figure 3 : Profile of U-component at the entrance of region 2

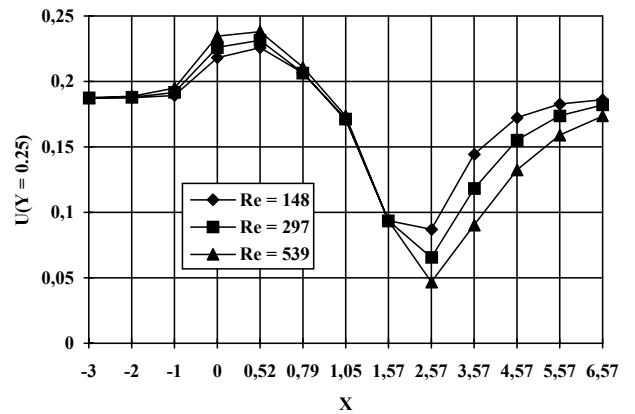


Figure 6 : Distribution of U-component along the channel

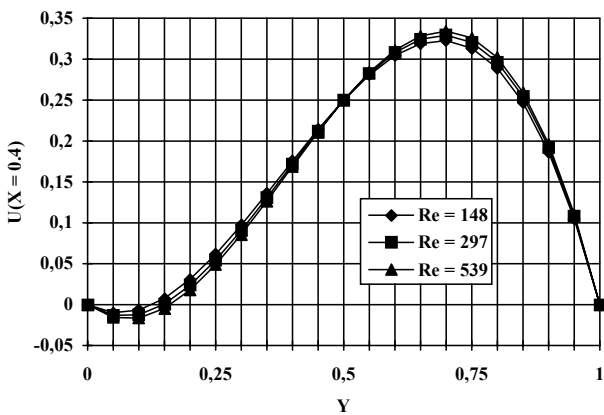


Figure 4 : Profile of U-component in bubble region

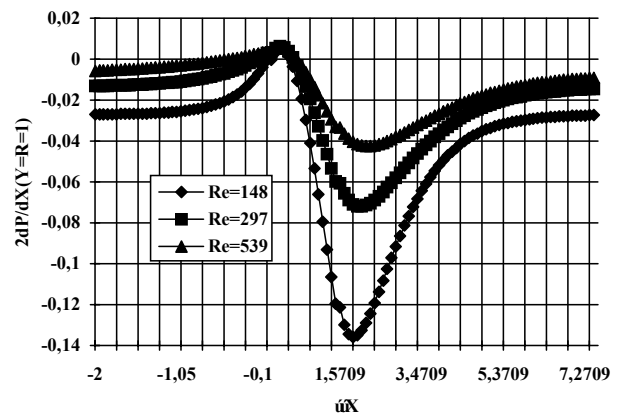


Figure 7 : Distribution of pressure gradient along the outer wall

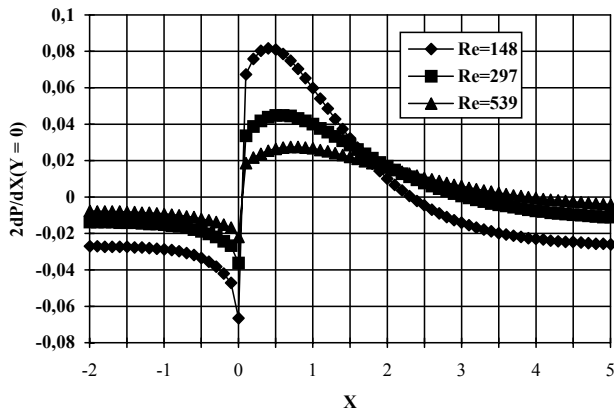


Figure 8 : Distribution of pressure gradient along the inner wall

Table 1 : Bubble length

L Re	Experimental results	Model results
148	1.111	1.100
297	1.611	1.556
539	2.166	2.118

**NOMENCLATURE**

- A,B = Constants
- F,G = Functions of Y
- H = dimensionless with channel (h/h)
- L = dimensionless bubble length (l/h)
- P = dimensionless pressure  $2p / \rho u^2$
- R = dimensionless radial coordinate (r/h)
- u = mean entrance flow velocity
- U = dimensionless axiale (tangential velocity component (u/u))

- V = dimensionless normal (radial velocity component (v/u))
- X = dimensionless abscissa (x/h)
- Y = dimensionless ordinate (y/h)
- Z = distortion function
- $\beta$  = angle of streamline deviation at the entrance of corner region
- $\theta$  = polar coordinate
- $\rho$  = fluid density
- $\gamma$  = kinematic viscosity
- Re = reynolds number (uh/ $\gamma$ )
- $r_i$  = inner curvature radius of the bend
- $r_e$  = outer curvature radius of the bend

**REFERENCES**

- [1] Manuscript on flow visualization and measurment Hugerup, H.J., Aero.Eng.Dep., R.P.I Troy N.Y U.S.A
- [2] Hurd, A.C.& Peters, A.R. 1970, Analysis of flow separation in a confined tow-dimensional channel, ASME Journal of Basic Engineering, Vol.92, pp.908-914
- [3] P. Orlandi & D.Cunsolo. 1979, Tow dimensional laminar Flow in Elbows, ASME Journal of Fluids Engineering, Vol.101, pp 276-283
- [4] G.Heskestad. 1971 Two-Dimensional Miter-Bend Flow, Journal of Basic Engineering, pp 433-439
- [5] A.M.K.P.Taylor & J.H.Whitelaw & M.Yinneskis. 1982 Curved Ducts With Strong Secondary Motion: Velocity Measurements of developing Laminar and Turbulent Flow, Journal of Fluid engineering Vol. 104, pp 350-358